International Journal of Materials Science and Technology Studies
ISSN: 3006-7693 (Print), ISSN: 3006-3744 (Online) | Volume 1, Number 1, Year 2024
DOI: https://doi.org/10.62051//ijmsts.v1n1.04
Journal homepage: https://wepub.org/index.php/IJMSTS/index

A study on aramid nano-aerogel fiber and its fabric thermal conductivity

Rui Fang[1], Yue Xie[1], Bo Zhang[2], Hao Wang[3], Min Zhang[4]

[1] School of Physical Science and Technology, Tiangong University, Tianjin 300387, China

[2] School of life Sciences, Tiangong University, Tianjin 300387, China

[3] School of Economic and Management, Tiangong University, Tianjin 300387, China

[4] School of Textile Science and Engineering, Tiangong University, Tianjin 300387, China

ABSTRACT

Aramid nano-aerogel represents an ideal structure for the fabrication of next-generation high-performance thermal insulation fibers and textiles. Single aramid nano-aerogel fiber can be achieved via wet spinning. The thermal conductivity of these fibers, a crucial determinant of textile insulation performance, remains under-explored in terms of numerical modeling. This research aims to establish a numerical inversion model to determine the thermal conductivity of single aramid nano-aerogel fiber. By simulating the three-dimensional geometry of plain fabric, the volume fraction of gas and solid within the fabrics are computed. Drawing from the law of energy conservation and Fourier's law of heat conduction, a relationship model is proposed between the thermal conductivity of single aramid nano-aerogel fiber and the overall thermal conductivity of the fabric. The finite difference method is employed to ascertain the thermal conductivity of single aramid nano-aerogel fiber. Furthermore, the influence of the geometric structure and the fiber diameter on the thermal insulation performance of the single-layer fabric is analyzed, which provides a feasible approach for the subsequent design of fabric structures with excellent thermal insulation properties.

KEYWORDS

Aramid nano-aerogel fiber; Fabric thermal conductivity; Structural model

1. INTRODUCTION

As the global warming phenomenon intensifies, the demand for sustainable and thermally insulating materials has escalated significantly [1]. Aerogel, possession of attributes such as ultra-low density, remarkable adsorption capabilities, and extensive surface area, has emerged as an exceptional thermal insulation material characterized by its exceptionally low thermal conductivity [2]. It can be used for the design and production of thermal protective textiles, encompassing fire-resistant clothing and high- and low-temperature-resistant work attire. The potential applications of aerogel span diverse fields such as aerospace engineering and high-temperature heat dissipation, thus highlighting its immense research significance and industrial relevance [3]. The thermal conductivity of single aerogel fibers serves as the fundamental parameter for understanding the thermal conductivity of aerogel fiber aggregates, providing the necessary basis for the development of textiles with specialized thermal properties. Furthermore, it lays the groundwork for the establishment of various aggregate thermal conductivity models rooted in the characteristics of aerogel fibers [4].

The determination of single-fiber thermal conductivity primarily encompasses two approaches: the direct method and the indirect method. The direct approach offers the direct measurement of the thermal conductivity of individual fibers using experimental equipment, thus mitigating potential errors associated with model equivalency and theoretical calculations. W. Yi [5] employed a 3ω testing system to directly assess the axial thermal conductivity and heat capacity of a carbon fiber specimen. Alternatively, J.L. Wang [6] utilized a variable-length "T"-shaped method to determine the apparent thermal resistance corresponding to distinct lengths of the identical fiber, subsequently deriving the thermal conductivity of asphalt-based carbon fibers and the associated contact thermal resistance at the junctions. H.Y. Dong [7] introduced the laser Raman technique for measuring the thermal conductivity of individual carbon fibers, comparing the results with those obtained using the DC power method to arrive at a more authentic representation of fiber thermal conductivity. Nevertheless, due to the significant length-to-diameter ratio and the minute diameter (below 100 micrometers) of single nano-aerogel fiber, the direct measurement of their thermal conductivity remains a highly challenging endeavor within the realm of physical testing. The thermal conductivity of single fiber is often estimated by constructing a heat transfer model for fiber aggregates. Although these models can provide insights into the thermal behavior of fibers, they are inherently subject to certain equivalent errors. L. Li [8] addressed this challenge by developing a specialized sample preparation technique for fibers. Using the Thermal Properties Analyzer (TPS), they measured the thermal conductivity of the composite system and subsequently derived the equivalent thermal conductivity of a single carbon fiber based on the series-parallel physical model of the two-phase composite medium. Z.L. Wang [9] and his colleagues took a different approach by formulating the axial heat conduction equation for a single carbon fiber, accounting for environmental heat losses. This approach allowed them to establish a relationship between the thermal parameters of the carbon fiber and the frequency domain characteristics of the AC heating signal. Y. Cai [10] took a numerical approach, developing a model to assess the equivalent thermal conductivity of each element within a material. This model integrated the series-parallel theory for the equivalent thermal conductivity of composite materials and considered the distribution of yarn and air in various regions of the tissue cycle and. However, the majority of existing research has focused on the thermal conductivity of single fibers within composite or porous materials. There is a dearth of studies examining the numerical computation of thermal conductivity for single aramid nano-aerogel, an area ripe for further exploration.

In the present investigation, a single aramid nano-aerogel yarn was meticulously prepared via wet spinning techniques, followed by the meticulous creation of a plain fabric using mechanical weaving methods. Subsequently, an interpolation and fitting procedure were employed to approximate central axis equation of aramid nano-aerogel fiber, enabling the generation of a three-dimensional geometric model that accurately represented the fabric's real structure. Lastly, utilizing the principles of conservation of energy and Fourier’s law of heat conduction, a comprehensive model was developed to elucidate the relationship between the thermal conductivity of an individual aramid nano-aerogel fiber and the overall thermal conductivity of the fabric. This model was solved using thermal analysis theory, incorporating the first-kind boundary value relationship and finite difference methods. Through this rigorous approach, the thermal conductivity of the individual aramid nano-aerogel fiber was valid predicted. Furthermore, by adjusting pertinent parameters, the study comprehensively examined the influence of fabric geometry and fiber thickness on textile insulation properties. This analysis offers a viable avenue for the optimization of fabric thermal performance, taking into account both macro- and micro-scale factors.

The novelty of this study lies in the establishment of a relationship model between the thermal conductivity of single aramid nano-aerogel fiber and the overall thermal conductivity of the fabric. This model offers a novel approach for measuring the thermal conductivity of single fiber within a nano-aerogel matrix. Additionally, the model's applicability extends beyond nano-aerogel materials, encompassing other porous and composite materials, thereby broadening its utility in thermal

conductivity measurements. In terms of practical implications, this study provides critical parameter support and theoretical underpinnings for the optimization of textile insulation properties. The findings of this investigation are expected to significantly impact the design and development of thermally efficient fabrics, thus contributing to advancements in the field of thermal insulation materials.

2. MATERIALS AND METHODS

2.1. Materials

Para-aramid fiber (PPTA) was purchased from Teijin, length 50mm, linear density 1.7 dtex. Dimethyl sulfoxide (DMSO, 99.7%) was provided by Tianjin Kemeou Chemical Reagent Co. Ltd. Sodium hydroxide (NaOH), potassium hydroxide (KOH), tertiary butyl alcohol (TBA), purchased from Tianjin Kairuisi Fine Chemical Co. Ltd.

2.2. Geometric description of fabric structure

Plain fabric is one of the most basic and common fabric structures in textiles. It consists of warp and weft yarns interlaced and woven in a 1:1 manner. Because of the presence of basic repeating units in the weave pattern, repeating cells or minimum period structures are often used to construct representative volume units in making thermal property predictions.

In fabric geometry modeling, the key parameters are yarn cross-sectional shape, yarn thickness, and distance between yarns. The degree of fiber curl varies according to these parameters. By wet spinning, we obtained aramid nano-aerogel fibers, which were further woven to obtain plain fabrics. The fabric geometric parameters are defined as follows: 1) ρ_s and ρ_w are the fabric warp and weft densities, respectively, yarns/mm; 2) d is the diameter of a single aramid nano-aerogel fiber; 3) θ_s and θ_w are the bending angles of the warp and weft yarns, respectively; 4) A is the upper surface area of the fabric repeating unit outside the outer rectangles; and 5) L is the height of the fabric outside the rectangles. Based on the optical microscope and Tracker software, we physically measured the warp and weft thicknesses of the plain fabric, and then calculated the tangent values of the corresponding warp and weft bending angles with the following equations:

$$\begin{cases} \tan\theta_s = \dfrac{d}{\frac{1}{\rho_s}} = d\rho_s \\ \tan\theta_w = \dfrac{d}{\frac{1}{\rho_w}} = d\rho_w \end{cases} \tag{1}$$

For the equations of the median axis of fibers, we take one median axis of the warp yarn (weft yarn) as an example to start the description. Considering the periodicity of yarn bending, we use the sinusoidal function to approximate the simulation of the periodic fluctuation of the warp (weft) yarn. Within a cycle, five reference points are selected as the endpoints for interpolation fitting. The specific selection scheme is as follows:

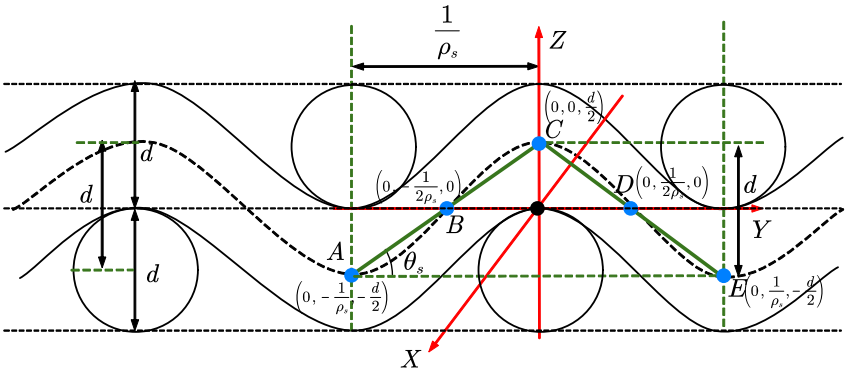

Figure 1. geometric figure

A three-dimensional right-angle coordinate system is constructed with one interweaving point of the warp and weft yarns as the origin. According to the parameters of the fabric geometric structure, the coordinates of the five points are $\left(0,-\frac{1}{\rho_s},-\frac{d}{2}\right)$, $\left(0,-\frac{1}{2\rho_s},0\right)$, $\left(0,0,\frac{d}{2}\right)$, $\left(0,\frac{1}{2\rho_s},0\right)$, $\left(0,\frac{1}{\rho_s},-\frac{d}{2}\right)$.

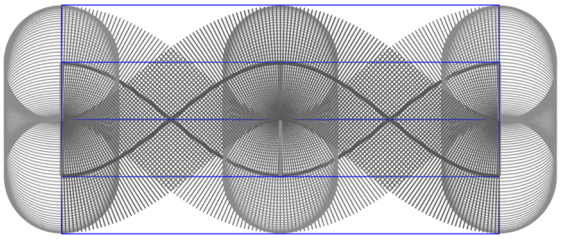

(a) Main view of the central axis

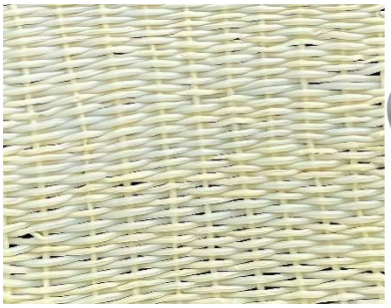

(b) plain weave fabric

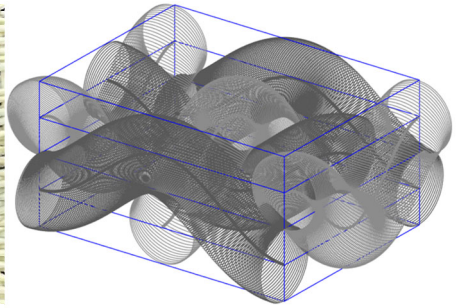

(c) idealized model

Figure 2. Physical and minimum repetition unit simulations of aramid nano-aerogel plain fabrics

Based on the five-point coordinates, the equations for the center axis of the fabric can be obtained based on sinusoidal interpolation fitting.

In this study, in order to reasonably simplify the computational difficulty, it is assumed that the cross section of the fibers is an undeformed circle and that there is a uniform thermal conductivity in the fibers [11]. Fig. 2 shows the physical figure of the aramid nano-aerogel plain fabrics, as well as the three-dimensional minimum repetitive unit simulated by the simulation approximation.

2.3. Theoretical Models of Fabric Heat Transfer

Fabric is a non-homogeneous material composed of fiber matrix and air [11], and its heat transfer is mainly by heat conduction, heat convection and heat radiation. Therefore, its total thermal conductivity Q is mainly composed of heat conduction Q_k, convective heat transfer Q_c and radiative heat transfer Q_c, which compliance with the law of energy conservation [12].

$$Q = Q_k + Q_c + Q_r \tag{2}$$

The test environment in this study is in a constant temperature and pressure experimental environment, and the fabric is covered by the experimental hood during the test, so the effect of natural convection on the experiment is not considered, $Q_c = 0$; The transient heating method is used to heat one side of the fabric, and the temperature gradient at the surface of the fabric is small, so the radiant heat transfer is negligible, $Q_r = 0$.

In the fabric heat transfer modeling study, the heat transfer along the fabric thickness direction can largely reflect the thermal insulation performance of the fabric, so this paper assumes that the heat released by the Hot Disk probe is only transferred along the thickness direction, and the effect of the lateral transfer of heat is negligible. Therefore, the fabric is regarded as a flat plate composed of fiber matrix and air, and only the heat transfer process in the thickness direction of the fabric is considered. Since the heating process starts from the initial state and the temperature of each point in the fabric changes with time, a one-dimensional non-stationary Fourier heat transfer model is established, which can be expressed as follows.

$$Q = A\lambda \frac{\partial T}{\partial x} \tag{3}$$

Where, A is the fabric unit surface area, mm^2; λ is the thermal conductivity, also known as the thermal conductivity coefficient, is a parameter reflecting the thermal insulation properties of the fabric, W/mK; is the unit of the fabric temperature difference between the upper and lower sides of the surface, K; ∂x is the unit of the thickness of the fabric.

In the process of thermal conductivity, the amount of heat per unit time through a given cross-section is proportional to the rate of change of temperature perpendicular to the direction of this cross-section and the cross-section area, the direction of heat transfer is opposite to the direction of the temperature rise, the heat flux of each direction within the fabric can be decomposed into x, y, z three axes of the direction of the diversion of the heat, according to the Fourier's law [13], can be expressed as follows.

$$\begin{cases} q_x = -\lambda \dfrac{\partial T}{\partial x} dydz \\ q_y = -\lambda \dfrac{\partial T}{\partial x} dxdz \\ q_z = -\lambda \dfrac{\partial T}{\partial x} dxdy \end{cases} \tag{4}$$

Where, q_x, q_y, q_z denotes the heat flow through the $y-z, x-z, x-y$ three microelement surfaces into the fabric microelement body. Since only the temperature change of the fabric in the thickness direction is considered, i.e., x, the direction, and there is no internal heat source inside the fabric, the heat conduction equation in the fabric can be expressed as follows.

$$\frac{\partial T}{\partial t} = a \frac{\partial^2 T}{\partial x^2} \tag{5}$$

Where, $a = \dfrac{\lambda}{\rho c_p}$ is the thermal diffusion coefficient, mm^2/s; ρ is the density of the fabric; c_p is the specific heat of the fabric, MJ/m^3K.

2.4. Boundary Conditions and Control Equations

While measuring the thermal conductivity of the fabric, Hot Disk probe can record the surface temperature of the fabric on the side near the heat source in real time, thus satisfying the first-kind boundary conditions. In this study, considering that the heat transfer process is non-stationary, there exists a moment when the heat flow is transferred to the other side of the fabric, so the approximate assumption is that the heat flow is transferred to the other side of the fabric in 0.1s, then the surface temperature of the fabric on the side far away from the heat source is constant as the room temperature 25℃, which satisfies the first-kind boundary conditions. The initial value of the temperature distribution inside and on the surface of the fabric is 298.15K. The boundary conditions are expressed as:

$$\begin{cases} T|_{x=0} = T_r \\ T|_{x=L} = T_0 \end{cases} \tag{6}$$

Where, $T|_{x=0}$ is the temperature of the side of the fabric in contact with the heat source; T_r is the surface temperature of the fabric on the side near the heat source, given by the value recorded by Hot Disk probe; $T|_{x=L}$ is the surface temperature of the fabric on the side away from the heat source; L is the overall thickness of the fabric; $T_0 = 25°C$ indicates the overall initial temperature of the fabric.

The law of energy conservation, as one of the basic rules for analyzing all heat transfer problems, is applicable to both steady state and unsteady state heat transfer problems. In view of the boundary conditions set above, the governing equation for the heat transfer performance of the fabric is given on the basis of conservation of energy as:

$$\rho c_p \mu \cdot \nabla T = \nabla(\lambda \cdot \nabla T) + q \tag{7}$$

Where, μ is the velocity vector, q is the fabric internal heat source. The fabric in this study does not consider the internal heat source, that is $q = 0$. Therefore, the increment of energy $\rho c_p \mu \cdot \nabla T$ of the fabric model per unit time is equal to the heat conducted $\nabla(\lambda \cdot \nabla T)$ through the volume boundary by thermal conduction from the boundary in contact with the heat source per unit of time.

2.5. Mesh Partitioning and the Finite Difference Method

The solution of the heat transfer problem is a high-dimensional nonlinear process, and the traditional analytical solution is complicated and cumbersome, so the same and continuous physical parameters in space and time are discretized and numerically solved using the finite difference method, which significantly reduces the computational error and improves the accuracy of the results [14]. On the basis of the one-dimensional unsteady heat conduction model, the time coordinate is introduced, so that the problem dimension becomes two-dimensional, including time $_t$ and space $_x$ variables. The temperature propagates unidirectionally with time, i.e., the former state has an influence on the latter state, and the latter state cannot influence the former state, as follows:

$$T_i^{k+1} = F_o^{k+1} T_{i-1}^k + (1 - 2F_o^{k+1}) T_i^k + F_o^{k+1} T_{i+1}^k \tag{8}$$

Where, $F_o = {}^{a\Delta t}/_{\Delta x^2}$, is called the Fourier coefficient; $i = 1, 2, .., k; k = 1, 2, .., 5$

As shown in Fig. 4 for the one-dimensional unsteady heat conduction problem with spatial and temporal partitioning.

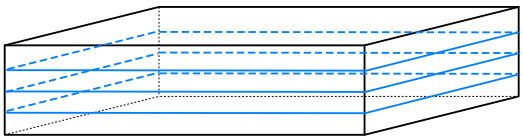

Figure 3. Discretization of the ideal fabric

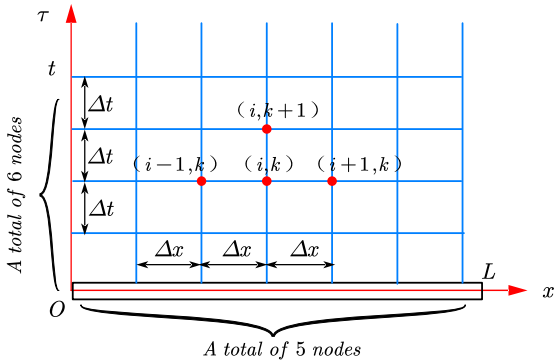

Figure 4. Grid partitioning

In the process of unsteady heat transfer, there is a nonlinear temperature field inside the fabric. The dense mesh division will have the problem of excessive model solution complexity and insufficient computational capability. To reduce the solution complexity, the 0.1s time period was divided into 6 groups, while the fabric was divided into 4 cells. Utilization of space step $\Delta x = L/N$, time step $\Delta t = t/M$ Separate the spatial interval [0, L] and temporal interval [0, t] into N, M equal parts. Where, N=5, M=6. Fig. 4 where i denotes the position of the node within the fabric and k denotes the $k\Delta t$ moment, for the inner node i, at the k and $k+1$ moments, Eqs. (5) exist.

$$\begin{cases} \left(\dfrac{\partial T}{\partial t}\right)_i^k = a\left(\dfrac{\partial^2 T}{\partial x^2}\right)_i^k \\ \left(\dfrac{\partial T}{\partial t}\right)_i^{k+1} = \left(\dfrac{\partial^2 T}{\partial x^2}\right)_i^{k+1} \end{cases} \tag{9}$$

Differential discretization of the partial derivative of temperature with respect to time at the left end of Eqs. (9), there exists:

$$\begin{cases} \left(\dfrac{\partial T}{\partial t}\right)_i^k = \dfrac{T_i^{k+1} - T_i^k}{\Delta t} \\ \left(\dfrac{\partial T}{\partial t}\right)_i^{k+1} = \dfrac{T_i^{k+1} - T_i^k}{\Delta t} \end{cases} \tag{10}$$

The above equation represents the first-order derivatives of temperature with respect to time for the forward and backward differences, respectively, where the truncation errors for both the forward and backward difference equations are first-order truncation errors $O(\Delta x)$.

By associating the forward differential equation in Eqs. (10) with the backward differential equation, there exist:

$$\left(\frac{\partial T}{\partial t}\right)_i^k = \frac{T_{i-1}^k - 2T_i^k + T_{i+1}^k}{\Delta x^2} \tag{11}$$

The above equation represents the second-order derivative of temperature with respect to x for the central difference equation, where the truncation error of the central difference equation is the second-

order truncation error $O(\Delta x^2)$, when Δx is small enough, the second-order truncation equation is more accurate than the first-order truncation equation, and the central difference equation is generally used for the solution calculation. For the unsteady heat conduction problem, the numerical solution will be unstable when applying the center difference equation with the first-order derivative of temperature with respect to time, so the forward difference and backward difference equations are used to express the first-order derivative of temperature with respect to time.

The unsteady heat conduction problem has display difference format calculation and implicit difference format calculation [15]. The use of implicit difference format calculation is required to use the calculation of the moment of temperature data. The display difference format can be recursive through the previous moment of temperature with a low workload. Based on this, the display difference format is used to solve the calculation of the one-dimensional unsteady heat conduction model. The diffusion term in the one-dimensional unsteady heat conduction equation (5) uses the center difference when the diffusion term is on the k+1 layer, and the unsteady term will T Use the forward difference at node $(i,k+1)$ for node (i,k) In summary there exists a system of equations for the computation of the display difference format:

$$\begin{cases} T_i^{k+1} = F_o T_{i+1}^k + (1-2F_o) T_i^k + F_o T_{i-1}^k \\ F_o = \dfrac{a\Delta t}{\Delta x^2} \\ a = \dfrac{\lambda}{\rho c_p} \end{cases} \tag{12}$$

Where, F_o is the number of Fourier numbers introduced, which is calculated in the display format by requiring $F_o < 0.5$, in which case the second law of thermodynamics is obeyed and the calculated value stabilizes at different moments; $i = 2, 3, .., N-1; k = 0, 1, 2, .., 5.$

2.6. Thermal conductivity inversion model of aramid nano-fibrous aerogels.

To address the difficulty of direct measurement of single aramid nano-aerogel fiber, an indirect method can be used to treat the fiber matrix and air as a fiber aggregate. The thermal conductivity of a single aramid nano-aerogel fiber is performed inversely by solving the effective thermal conductivity of the fiber aggregate. Based on different combination rules, there are five main types of structural models that can be used to calculate the effective thermal conductivity of porous material fibers. These models include series, parallel, two models based on Maxwell-Ocken theory and effective medium theory (EMT) [11]. In this study, we have chosen the simplest two-phase parallel model to represent the effective thermal conductivity of a two-component fiber aggregate λ_{eff}, as follows:

$$\lambda_{eff} = \sigma\lambda_s + (1-\sigma)\lambda_g \tag{13}$$

Where, λ_s is the thermal conductivity of a single aramid nano-aerogel fiber, W/mK; λ_g is the thermal conductivity of static air between fibers, W/mK; σ is the fiber volume occupancy in the cell, It can be obtained from the three-dimensional minimum repeating unit obtained in 2.2 based on the microelement method. The following figure shows the division of the repeating unit.

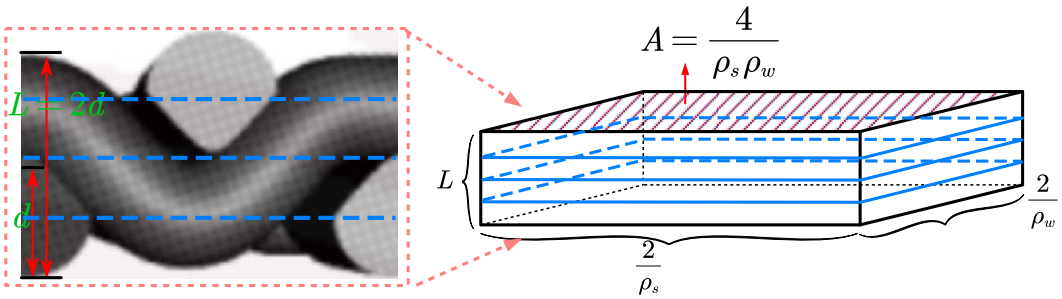

Figure 5. Discretization of fabric repeating units

Firstly, a single yarn consisting of points is obtained by discretizing each circular section of a single fiber into a number of points. Secondly, the outer rectangle of the smallest fabric unit is discretized based on equal discrete intervals. Ultimately, when the corresponding point (x_i, y_i, z_i) of the warp and weft yarns after the ith micro-element lies within the closed range formed by the discrete points (x, y, z) of the eight boundary points of the cube, the point is considered to be a valid point inside the repeating unit representing the fiber matrix, which can be expressed by the following equation:

$$(x_{i_{fabric}}, \quad y_{i_{fabric}}, \quad z_{i_{fabric}}) \in \begin{pmatrix} x_1, & y_1, & z_1 \\ \vdots & \ddots & \vdots \\ x_8, & y_8, & z_8 \end{pmatrix} \tag{14}$$

According to the above method, the total volume of fiber matrix and air can be approximated by the number of points in the rectangle containing the total, V_{sum}; The volume occupied by the fiber matrix can be approximated by the number of points obtained by discretizing the yarn in the smallest repetitive unit, V_{sum}; According to the statistical principles, it can be calculated that $\sigma = V_s / V_{sum}$.

Next, we further analyze the relationship between temperature per unit of fabric and thermal conductivity.

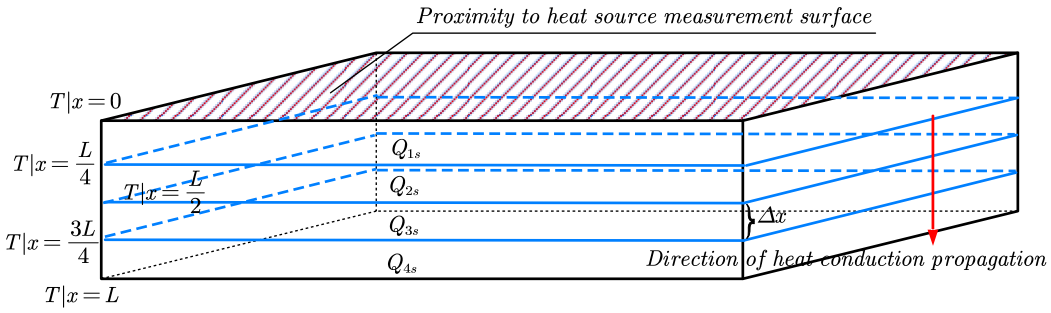

Figure 6. Temperature and heat flux distribution map of the fabric unit

At the initial moment, the surface and internal temperatures of the unit fabric are $25°C$, the surface temperature of the side close to the heat source changes within 0.1s, and the temperature of the unit fabric also changes, the unit ideal fabric is discretized into 4 layers. For the thickness of the layer:

$$\Delta x = \frac{L}{4} = \frac{d}{2} \tag{15}$$

Where, Δx is the thickness of each fabric layer, mm. After dividing the unit, according to the principle of heat transfer, the overall thermal conductivity Q_{ms} of the fiber matrix and the static air between the fiber gaps in each layer of the unit can be calculated separately. The sum yields the total heat conductivity of the repeating unit, Q_{st}.

$$\begin{cases} Q_{st} = \sum_{m=1}^{4} Q_{ms} \\ Q_{ms} = \lambda_{eff}^{m} A \dfrac{\Delta T_m}{\Delta x} \end{cases} \tag{16}$$

Where, $m = 1, 2, 3, 4$; λ_{eff}^{m} is the equivalent thermal conductivity of the single A-fiber per layer and of the static air between the fiber voids, W/mK; A is the surface area on the repeating unit of the fabric, m^2. It can be calculated from the warp and weft densities, i.e., $A = \dfrac{4}{\rho_s \rho_w}$.

On this basis, according to the law of energy conservation, a model can be constructed for the relationship between the thermal conductivity of the overall fabric and the thermal conductivity of single aramid nano-aerogel fiber, and the minimum error term can be introduced:

$$\min |\delta| = |Q_{zt} - Q_{st}| \tag{17}$$

where, Q_{zt} is the unit fabric thermal conductivity, W; Q_{st} is the static air thermal conductivity between single aramid nano-aerogel fiber and fiber voids, W; δ is the error term, which indicates the error between the true value of the repeated unit thermal conductivity and the predicted value. When $|\delta|$ tends to infinity, the inverse deduced thermal conductivity of a single aramid nano-aerogel fiber is the optimal result.

In summary, the relationship model between the thermal conductivity of a single aramid nano-aerogel fiber and the thermal conductivity of the fabric is as follows:

$$\min \delta = |Q_{zt} - Q_{st}| \tag{18}$$

$$\begin{cases} Q_{zt} = \sum \lambda_z A \dfrac{(T_{zi}^6 - T_{z(i+1)}^6)}{\Delta x} \\ Q_{st} = \sum \lambda_{eff} A \dfrac{(T_{si}^6 - T_{s(i+1)}^6)}{\partial x} \\ Q_{zt} = Q_{st} \end{cases} \tag{19}$$

2.7. Algorithm Design

After discretizing the one-dimensional non-steady-state heat transfer model using the finite difference method, based on the established boundary conditions and initial values, layer-wise discretization is performed at different time and space nodes. This establishes the relationship between unknown values and the temperature values on the fabric's heat source side, and constructs a model for the relationship between the overall thermal conductivity of the fabric and the thermal conductivity of a single aramid nano-aerogel fiber. Consequently, the thermal conductivity of the fabric is searched for relative to the thermal conductivity of a single aramid nano-aerogel fiber. Given the overall thermal conductivity of the fabric, the algorithm for calculating the thermal conductivity of a single aramid nano-aerogel fiber is designed as follows:

Step 1: Set the fabric structure parameters and determine the boundary conditions and initial conditions of the heat conduction model.

Step 2: Discretize the unit fabric using the finite difference method, and calculate the heat conduction of the fabric through the overall thermal conductivity of the fabric.

Step 3: Search for the thermal conductivity of a single aramid nano-aerogel fiber within the interval [0.02624, 1] with a step size of 0.00001.

Step 4: Output the optimal value of the thermal conductivity of a single aromatic polyamide nanofibrous aerogel fiber when the error term δ is minimized.

3. RESULTS AND DISCUSSION

3.1. Thermal Conductivity of Single Aramid Nano-aerogel Fiber

The geometric structure parameters of the fabric can be acquired using the optical microscope and the Tracker program in the manner described below:

Table 1. Geometric structural parameters

Type	Fiber diameter/mm	Warp density yarns/mm	Weft density yarns/mm
Plain weave	0.436	0.8333	0.625

The internal fiber matrix occupancy and static air occupancy of each cell in the minimal periodic structure of plain-weave fabric can be computed using the Eqs. (14) In conjunction with the structural parameters listed in Table 1, as indicated in the table that follows:

Table 2. The distribution tables of occupancy rate

Occupation rate	Layer 1	Layer 2	Layer 3	Layer 4
Air	0.8519	0.6386	0.6462	0.8524
Fiber matrix	0.1481	0.3614	0.3538	0.1476

The calculated fiber matrix volume includes both the static air inside and the nano-aerogel fibers since we calculate the thermal conductivity of a single aramid nano-aerogel fiber as a uniform whole. As a result, the final fiber matrix's proportion is significantly higher than that of the nanofibers of the actual aerogel. Furthermore, the Hot Disk software test may determine the fabric's thermal conductivity and the associated thermal performance metrics, as indicates in the following table:

Table 3. Thermal properties of fabrics

Thermal conductivity of fabrics W/mK	Specific heat capacity MJ/mK	Thermal diffusivity mm^2/s
0.0332	0.05	0.663

Lastly, the problem is resolved using the inversion model in accordance with the design approach in 2.7. The findings demonstrated that, in accordance with theory, a single aramid aerogel fiber's thermal conductivity was 0.05624W/mK. This is because the fabric is really an air-and fiber-matrix-based fiber aggregate. It has a known static air thermal conductivity of 0.02624W/mK and a total thermal conductivity of 0.0332W/mK. Furthermore, the vacuum has a thermal conductivity that is marginally higher than that of the stagnant air. it indicates that the material has superior thermal-insulating capabilities. According to the thermal resistance theory, there is a weighting coefficient ratio between the thermal conductivity of air and aramid nano-aerogel fibers when calculating the equivalent thermal conductivity of fabrics. As a result, the expected results should be greater than or equal to the thermal conductivity of fabrics, with a small change range.

3.2. Analysis of influencing factors of heat transfer

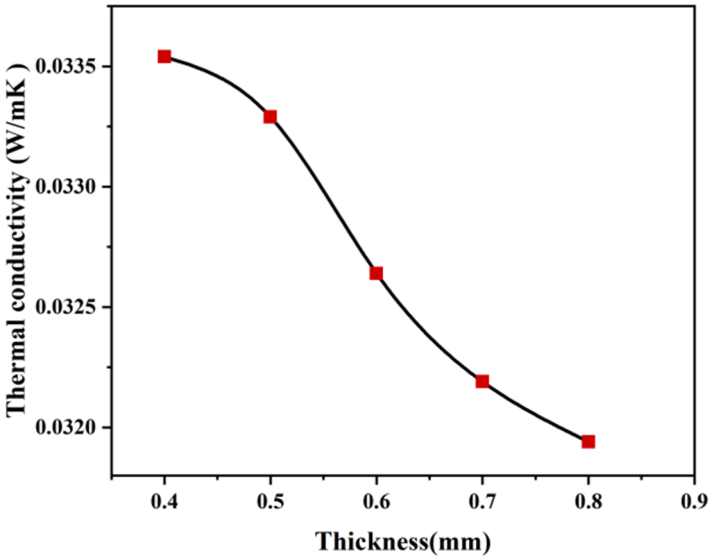

Figure 7. Correlation between the thermal conductivity fabric and fiber thickness

With a constant number of threads, the fabric's thermal conductivity rises as thickness grows and exhibits an inverse S-shaped growth curve, meaning that the rate of thickness increase initially increases and then decreases. The third law of thermodynamics states that heat conduction is the process by which heat moves from a high temperature to a low temperature. Static air and the fiber matrix will prevent heat transfer from occurring as it moves through the fabric's thickness. The heat transmission path and the fabric's thermal resistance both increase with the diameter of the fiber, improving the insulating properties of the material. Nevertheless, the fabric's thermal conductivity tends to become flat when thickness increases beyond a certain point. This is because as fabric thickness increases, a significant volume of still air inside aramid nano-aerogel fibers becomes active. This enhances airflow between the pores in the fabric, increasing convective heat transfer and impacting the fabric's ability to block heat while decelerating the trend of decreasing thermal conductivity.

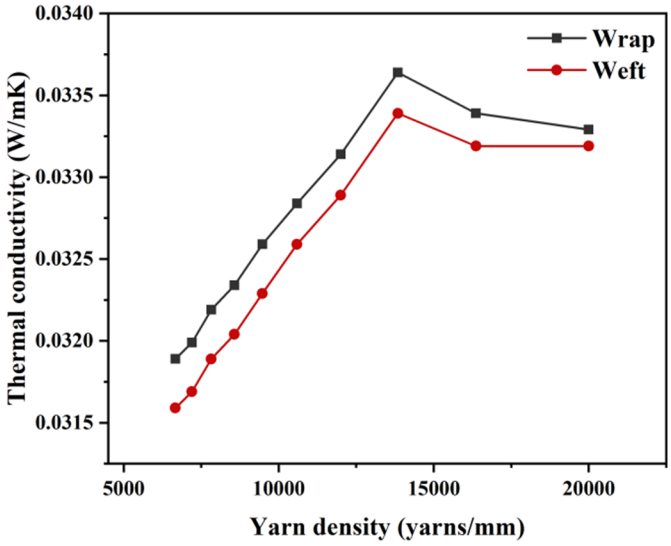

Figure 8. Correlation between the thermal conductivity fabric and density of the warp (weft)

After determining the thickness of the fabric, we can modify the yarn's warp and weft densities to alter how tightly the yarn is arranged. Fig 8 illustrates how increasing either the warp density or the weft density causes the fabric's tightness to rise and the distance between its two adjacent warp (or weft) yarns to shrink, which lowers the amount of air in the fabric structure. The fabric's thermal

conductivity increases first and then declines with an increase in warp (weft) density; In other words, it increases initially and then falls. This is because the thermal conductivity of the fiber matrix and the air both affect the fabric's thermal conductivity. However, this article makes the assumption that the fabric's pores are filled with static air, which means that air has superior thermal insulation than aramid nano-aerogel fibers and that the decrease in air volume occupies results in worse thermal insulation. As the density of the warp (weft) increases, the distance between two adjacent fabrics becomes less than that of a single aramid nano-aerogel fiber. This results in a significant compression set between distinct yarns, hence invalidating the concept of fabric circularity. Since the fabric thickness varies concurrently with the unestablished prerequisites of the control variable approach, the abnormal reduction of the interval [13850,20000] is not taken into consideration.

4. SUMMARY AND PROSPECT

This study focuses on the analysis of fabric geometry parameters and aerogel fiber diameters. Utilizing the five-point method and sinusoidal function fitting, a three-dimensional geometric model of the fabric is constructed. Drawing from the principles of heat transfer theory, a relationship model was established between the thermal conductivity of single aramid nano-aerogel fiber and the overall thermal conductivity of the fabric. Subsequently, adhering to the law of energy conservation, a solution strategy for determining the thermal conductivity of single aramid nano-aerogel fiber was devised. This approach offers a viable prediction scheme for assessing the thermal conductivity of single aerogel fiber comprising diverse materials, effectively addressing the challenges associated with current physical testing methodologies.

Furthermore, an investigation into the factors influencing the heat insulation performance of fabrics was conducted using the controlled variable method. (1) It was observed that as the thickness of the fabric increased while all other parameters remained constant, the thermal conductivity gradually decreased. However, once the thickness reached a certain level, the rate of decrease in thermal conductivity slowed significantly. (2) With a fixed fabric thickness, an increase in warp (weft) density resulted in an elevation of the fabric's thermal conductivity. It is worth noting that the warp (weft) density cannot be indefinitely increased as this would lead to the compression of aerogel fibers, subsequently altering the thickness and potentially compromising the heat insulation performance of the fabric.

Based on the aforementioned numerical solution model and analysis of influencing factors, this study provides a reliable research direction for further optimizing the design of fabric structures with excellent thermal insulation performance.

ACKNOWLEDGEMENTS

This work was supported by National College Students' innovation and entrepreneurship training program of Tiangong University (202310058016, 202310058030).

REFERENCES

[1] S. Schiavoni, F. D. Alessandro, F. Bianchi, and F. Asdrubali, "Insulation materials for the building sector: A review and comparative analysis" Renew Sust Energ Rev. 5(45), 988-1011 (2016).

[2] F. Zhu, and Y. Li, "Theoretical prediction and experimental characterization of radiative properties and thermal conductivities of fibrous aramid fabrics" J Ind Text. 51(5), 8826-8844 (2022).

[3] T. Xie, Y. L. He, M. Wu, and C. He, "A review of heat transfer models of nanoporous silica aerogel insulation material" J Eng Thermophys-rus. 35(2), 299-304 (2014).

[4] W. J. Li, H. R. Liang, Z. W. Zhang, J. Huang, H. M. Huang and J. Liang, "Analysis of influence of fabric architecture and radiation characteristics on effective thermal conductivity of carbonized woven thermal protection composites", Acta Astronautica. 188(3), 387-399(2021).

[5] L. Lu, W. Yi, and D. L. Zhang, "3ω method for specific heat and thermal conductivity measurements" *Rev Sci Instrum.* 72(7), 2996–3003 (2002).

[6] J. L. Wang, M. Gu, W.G. Ma, X. Zhang, and Y. Song, "Measurement of thermal conductivity of an individual fiber using changing length t-type method" J Eng Thermophys-rus. 12(26), 90-92 (2009).

[7] Y. D. Hu, J. H. Liu, H. D. Wang, and X. Zhang, "Simultaneous measurement of thermal properties and convective heat transfer coefficient of individual carbon fiber using Raman spectroscopy" CIESC Journal. 65(S1), 251-257 (2013).

[8] L. Li, H. Xiao, B. W. Cheng, and X. B. Kui, "Review of thermal conductivity of single fibers and their aggregates" J Silk. 53(08), 20-25 (2016).

[9] Z. L. Wang, D. W. Tang, X. H. Zheng, W. F. Bu, and W. G. Zhang, "Simultaneous measurements of thermal conductivity, thermal capacity of an individual carbon fiber" J Eng Thermophys-rus. 28(3), 490-492 (2007).

[10] Y. Cai, Y. C. Yang, and J. R. Qian, "Conductivity of Woven Fabrics Based on Structural Parameters" Adv Text Technol. 29(2), 43-49, (2021).

[11] D. Neda, P. Pedram, and T. Shahram, "Introducing a novel model for predicting effective thermal conductivity of spacer fabrics based on their structural parameters" J Therm Anal Calorim. 147(12), 6615-6629, (2022).

[12] P. Duda, "Heat Transfer Coefficient Distribution-A Review of Calculation Methods" Energies. 16(9), 1996-1073, (2023).

[13] H. D. Wang, B. Y. Cao, Z. Y. Guo, "Non-Fourier Heat Conduction in Carbon Nanotubes" J. Heat Transfer. 134(5), 0022-1481, (2012).

[14] S. Mazumder, "Comparative Assessment of the Finite Difference, Finite Element, and Finite Volume Methods for a Benchmark One-Dimensional Steady-State Heat Conduction Problem" J. Heat Transfer. 135(7), 0022-1481, (2017).

[15] S. Kazem, M. Dehghan, "Application of finite difference method of lines on the heat equation" Nemer Meth Part D E. 34(2), 0749-159X, (2018).

[16] L. Li, H. Xiao, B. W. Cheng, "Influence Factor and Study Status of Fabric Contact Warm-cool Feeling" Cotton Text Tech. 44(1), 80-84, (2016).